China Geology 6 (2023) 216–227

China Geology

Journal homepage: http://chinageology.cgs.cn
https://www.sciencedirect.com/journal/china-geology

Unraveling the mechanisms underlying lake expansion from 2001 to 2020 and its impact on the ecological environment in a typical alpine basin on the Tibetan Plateau

Chang-chang Fu[a, b,*], Xiang-quan Li[a, b,*], Xu Cheng[c]

[a] *Institute of Hydrogeology and Environmental Geology, Chinese Academy of Geological Sciences, Shijiazhuang* 050061, *China*
[b] *Key Laboratory of Quaternary Chronology and Hydrological Environmental Evolution, China Geological Survey, Shijiazhuang* 050061, *China*
[c] *Airborne Survey and Remote Sensing Center of Nuclear Industry, Shijiazhuang* 050000, *China*

ARTICLE INFO

Article history:
Received 11 June 2022
Received in revised form 5 December 2022
Accepted 22 March 2023
Available online 5 April 2023

Keywords:
Attribution analysis
Budyko framework
Climate change
Lake expansion
Water balance
Diverting water to the Yangtze River
Hydrogeology survey engineering
Tibetan Plateau

ABSTRACT

Yanhu Lake basin (YHB) is a typical alpine lake on the northeastern Tibetan Plateau (TP). Its continuous expansion in recent years poses serious threats to downstream major projects. As a result, studies of the mechanisms underlying lake expansion are urgently needed. The elasticity method within the Budyko framework was used to calculate the water balance in the Yanhu Lake basin (YHB) and the neighboring Tuotuo River basin (TRB). Results show intensification of hydrological cycles and positive trends in the lake area, river runoff, precipitation, and potential evapotranspiration. Lake expansion was significant between 2001 and 2020 and accelerated between 2015 and 2020. Precipitation increase was the key factor underlying the hydrological changes, followed by glacier meltwater and groundwater. The overflow of Yanhu Lake was inevitable because it was connected to three other lakes and the water balance of all four lakes was positive. The high salinity lake water diverted downstream will greatly impact the water quality of the source area of the Yangtze River and the stability of the permafrost base of the traffic corridor.

1. Introduction

With an average elevation of more than 4000 m, the TP and its surroundings contain the greatest ice reserves outside the Antarctic and the Arctic (Yao TD et al., 2012), and its lake area makes up roughly half of all the Chinese lakes. It is referred to as the "Asian Water Tower" because it is the source of more than 10 significant Asian rivers, including the Yangtze River, the Yellow River, and the Yarlung Zangbo (Immerzeel WW et al., 2010). In the "Third pole" region, where the "Asian Water Tower" is located, a significant volume of freshwater resources is stored, having a significant impact on social stability, human survival, and economic growth (Pritchard HD et al., 2019).

Global warming has reached previously unheard-of levels on earth over the past 50 years. The TP is at the region of the "Third pole" which is where global warming is most pronounced. In the context of global warming of 0.17°C per 10 years, the warming rate of this region is as high as 0.3°C to 0.4°C every 10 years, which is double the average of other locations in the world during the same period (Chen DL et al., 2015). The "Asian water tower" is changing dramatically in the context of fast global warming (Yao TD et al., 2019; Wang LC et al., 2021; Zhu L et al., 2022), displaying the features of an overall water imbalance, with lake expansion being one of the most important indicators.

With a combined area of 46500 km^2, the lakes on the "Asian Water Tower" make up 57.2% of China's total lake area (Zhang GQ et al., 2019). A large increase in the number of "Asian water tower" lakes was seen on the TP, and more than 80% of these lakes were growing, according to the second thorough scientific examination (Zhang GQ et al., 2019). Significantly, lakes supplied by glacier meltwater expanded more than non-glacier meltwater-fed lakes (Qiao BJ et al., 2019a). In terms of spatial distribution, the lake level in the inner flow area grew significantly, whereas the lake level primarily declined in the Yarlung Zangbo River basin (Biskop S et al., 2015; Qiao BJ et al., 2019b). Currently, the Tibetan Plateau's lakes experience an annual increase in water volume

First author: *E-mail address*: fuchangchang@mail.cgs.gov.cn (Chang-chang Fu).

* Corresponding author: *E-mail address*: fuchangchang@mail.cgs.gov.cn (Chang-chang Fu); lixiangquan@mail.cgs.gov.cn (Xiang-quan Li).

Literary editor: Xi-jie Chen
doi:10.31035/cg2023015
2096-5192/© 2023 China Geology Editorial Office.

of roughly 8 Gt, with about 26% of the increase coming from glaciers and permafrost melting (Zhang GQ et al., 2017).

The Hoh Xil region has the highest density of salt lakes in the world and is situated in the hinterland of the TP. This region is generally 4500 m above sea level in elevation. According to monitoring data, since 2000, this region on the TP has experienced some of the greatest warming and humidification (Wang C et al., 2022). Lakes in this region have kept growing as a result of climate change. The Qinghai-Tibet Railway and the Qinghai-Tibet Highway, which are of paramount importance, are located in the lower reaches of this region. The spilled lake water may have an impact on the downstream Yangtze River source's ecological environment and water quality, as well as thicken the active layer of frozen soil in the flowing area (Wu QB et al., 2013). In turn, this will wreak havoc on projects in frigid regions, including the Qinghai-Tibet Highway and the Qinghai-Tibet Railway, which rely on a cooling foundation as their primary method of construction (Yao XJ et al., 2018). Therefore, this area provides the perfect setting for research on the interactions between climate change, the environment, and water resources. In this study, the YHB was selected as the research area and the main objectives of this study are: (1) to analyze the trends in the lake area, river runoff depth, precipitation, and potential evapotranspiration, (2) to quantify the contributions of climate change and changes in underlying catchment properties to lake expansion and runoff increase since 2000, and (3) to discuss the potential impacts on the ecological environment of the diverting lake water to the Yangtze River.

2. Study area

The YHB is at 35°20′–35°50′ N, 91°30′–93°30′ E. It covers 8661 km^2 and lies between 4400–4800 m above sea level. The Kunlun Mountains form its northern boundary, and the Chumaer River forms its southern boundary. Goradanton Glacier on the TP is the source of the Yangtze River; in the Yangtze River source region, the southern tributary is referred to as the Tuotuo River and the northern tributary is referred to as the Chumaer River. The Qinghai-Tibet Highway and Qinghai-Tibet Railway are the major arteries of Tibetan transport, and they are about 10 km downstream of Yanhu Lake (Fig. 1).

There are four lakes in the basin, namely Zhuonai Lake, Kusai Lake, Haiding Noir Lake and Yanhu Lake from west to east. Historically, they were isolated from each other and were considered internal drainage systems. Furthest to the west is Zhuonai Lake, which has a surface area of 260 km^2; to the east of Zhuonai Lake is Kusai Lake (266 km^2) and Haiding Noir Lake (43 km^2); Yanhu Lake is furthest to the east which has an area of 45 km^2. The tributaries of the Yanhu Lake are all distributed in the north of the lake, including the Beiyi River, Bei'er River and Beisan River from west to east, which are all rivers mainly supplied by glacier meltwater. Because TP is becoming warmer and wetter, the four lakes have all expanded to varying degrees since 2000 (Figs. 2a–c). In 2011, Zhuonai overflowed. The lake area decreased sharply by approximately 115 km^2. The excess lake water was discharged downstream. Downstream, Kusai, Haiding Noir, and Yanhu were impacted directly. The area of Kusai increased rapidly from 286.3 km^2 on 22 August 2011 (before the outburst) to 332.1 km^2 on 19 August 2012 (after the outburst), and then remained stable between 2012 and 2018 (Fig. 2c). The area of Yanhu Lake expanded from 43.9 km^2 in 2010 to 207.6 km^2 in 2020 (Figs. 2a–b), which posed a great threat to the downstream. In this context, the hydrological and environmental geological surveys are carried out (Fig. 2d).

The study area is in the transition zone between the arid and semi-arid zones on the TP. Annual precipitation is between 100 mm and 500 mm. Precipitation is highly seasonal with approximately 90% of the annual precipitation falling during the summer monsoon season between May and September. The average annual temperature is −5.7°C and the average monthly temperature between October and April is below 0°C. Vegetation is generally sparse and dominated by alpine meadow grass.

The daily meteorological data of Wudaoliang and Tuotuohe stations between 1960 and 2020 were obtained from China Meteorological Data Service Centre (http://data.cma.cn/). These include precipitation, sunshine duration, wind speed, relative humidity, and mean, maximum and minimum air temperatures. The annual lake area in YHB between 1980 and 2020 was estimated using data from Landsat and Chinese high-resolution satellites and normalized the difference water index with an optimal threshold determined from the Otsu method (Otsu N, 1979). The glacier data was from the Chinese Glacier Inventory, which is supported by the National Cryosphere Desert Data Center of China (https://www.crensed.ac.cn/).

3. Methods

3.1. Trend test and breakpoint analysis

In the current study, the significance of the trends in annual meteorological and hydrological time series was estimated by using the nonparametric Mann-Kendall test at a significance level of 0.05 (Abdollah P et al., 2019). The Durbin-Watson (DW) test was used to remove the auto-correlation before executing the trend analysis (Mukhtar MA, 1987). The slope (β) of the trend was estimated (Sen PK, 1969) and a positive β value indicates a positive trend, i.e., an increase over time, and a negative β value indicates a decrease over time. Breakpoints were detected using the Mann–Kendall mutation test. The breakpoint was defined as the intersection between the statistical UF and UB curves. It is within the critical value range defined by a 0.05 significance level which is ±1.96.

3.2. Water balance

In the study area, the water balance of the closed lake can be expressed as:

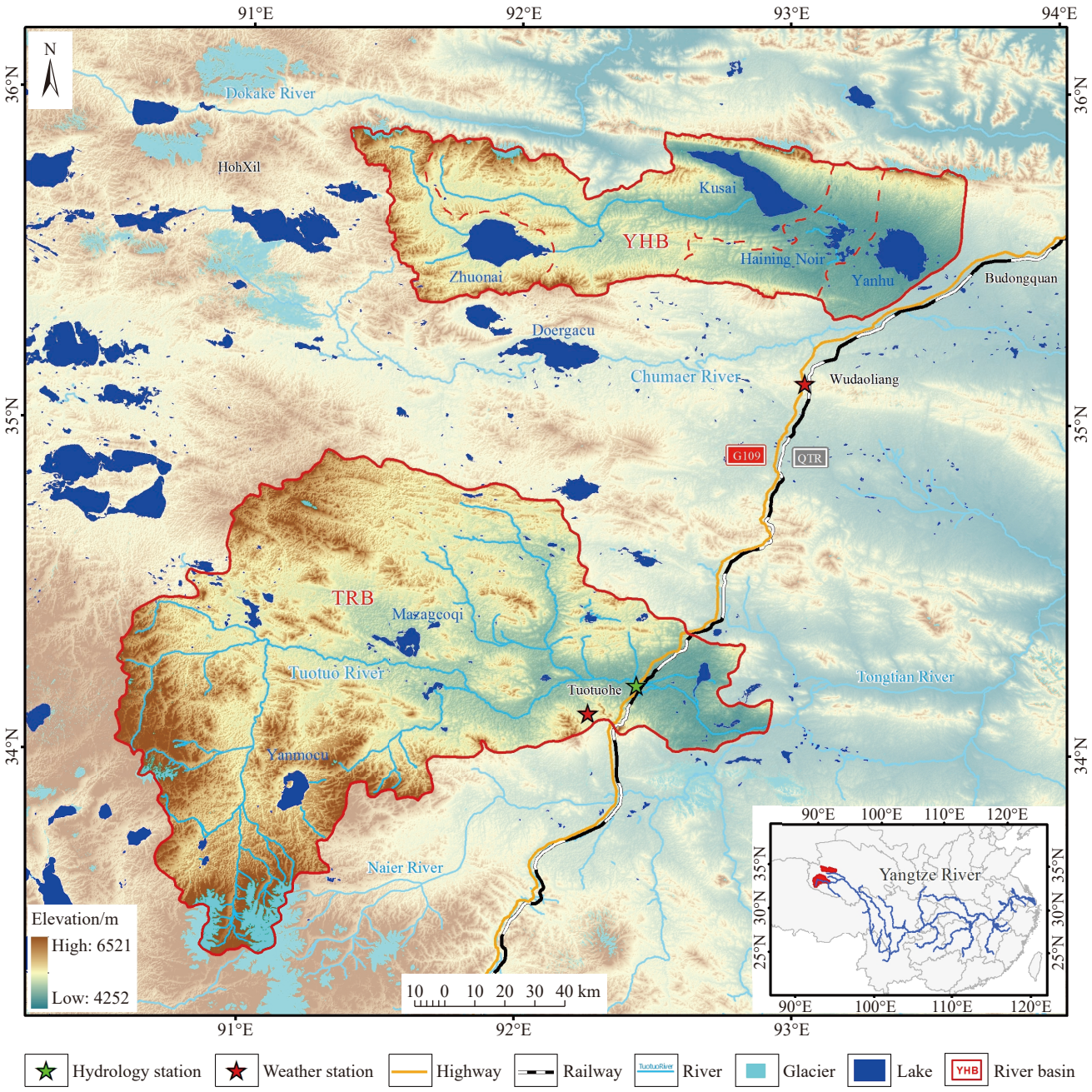

Fig. 1. Location and key features of the YHB and TRB. The illustration shows that the YHB and TRB are distributed in the source region of the Yangtze River.

$$\Delta V = P + R_L + G + GW - E \quad (1)$$

where ΔV is lake volume change, P is precipitation over the lake water surface, R_L is precipitation-induced land runoff, G is glacier meltwater, GW is groundwater input and/or output, and E is evaporation over the lake water surface.

The water level and lake area were used to calculate ΔV; P is the product between precipitation and the lake area; R_L is the product between land surface area and the difference between precipitation and actual evapotranspiration (E_a); G was calculated using an empirical formula; E is the product between evaporation over open water (ET_0) and the lake area. Using Eq. (1), the amount of GW was derived, which mainly originates from permafrost melt. In the YHB, the lake is the drainage base level in the basin, and the groundwater supplies the lake water, which is also an important reason why the lakes in this dry area can maintain a large lake surface area all year round (Yu et al., 2022).

(1) Evaporation over open water (ET_0)

Because of the lack of long-term data on lake evaporation in the study area, evaporation over open water was substituted with potential evapotranspiration (ET_0) (Rosenberry D et al., 2007; Zhou J et al., 2015). Following the Penman equation, open water evaporation was estimated as follows (Penman HL, 1948; Allen RG et al., 1989):

$$ET_0 = \frac{\Delta}{\Delta+\gamma}\frac{(R_n - G)}{\lambda} + \frac{\gamma}{\Delta+\gamma} f(u)(e_s - e_a) \quad (2)$$

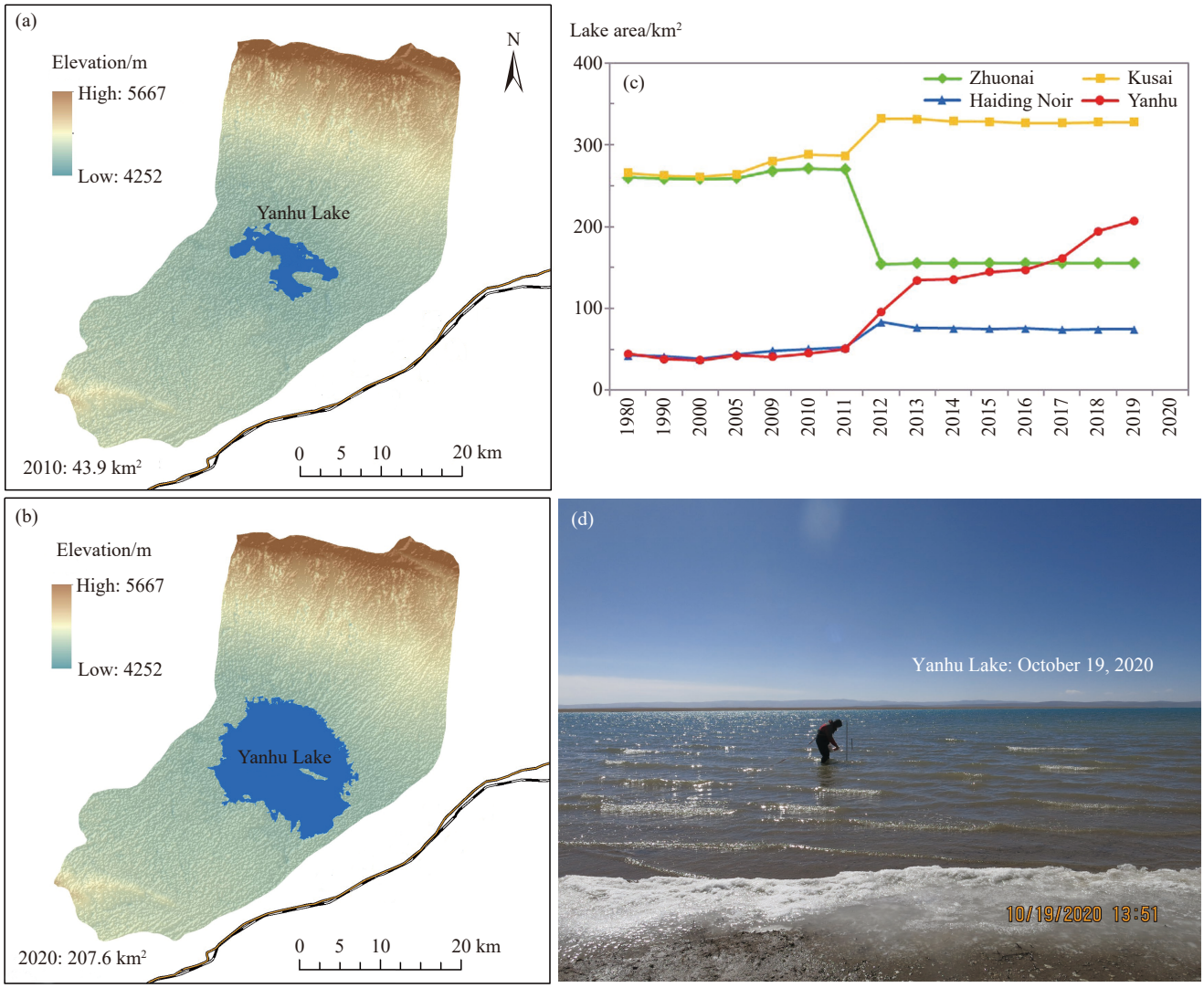

Fig. 2. Yanhu Lake area in (a) 2010, and (b) 2020; (c) interannual variations in areas of the four lakes; (d) the survey of water level and quality on October 19, 2020.

where ET_0 is the daily open water evaporation (mm/d); R_n is the net radiation at the water surface (MJ/m^6/d); G is the daily change in the heat storage of the water body; Δ is the slope of the saturation vapor pressure and temperature curve (kPa/°C); γ is the psychrometric constant (kPa/°C); λ is the latent heat of vaporization (MJ/kg); f(u) is a wind function typically of the form f(u)=a+bu, in which u is the wind speed measured at 2 m above the water surface, a and b are the fraction of extraterrestrial radiation reaching the earth; e_s–e_a is the vapor pressure deficit (kPa), e_s is the saturation vapor pressure for a given period (kPa), while e_a is the actual vapor pressure (kPa). Details on the implementation of the equation can be found in Zhou J et al. (2015).

(2) Volume of glacier meltwater

The following empirical formula was used to estimate the volume of glacier meltwater: V_g=0.042×$S_g^{1.3565}$ (R^2=0.9998), where S_g is the glacier area and V_g is the glacier volume. The formula was derived from the data of 253 glaciers distribute in the surrounding area in the China Glaciers Catalogue (Shi YF et al., 2003). Using remote sensing images, the changes in glacier area and volume was estimated. The volume of glacier meltwater is the product of glacier volume change and 0.9. According to drilling data, the study area is covered by permafrost that extends to a maximum depth of 2–3.5 m. Therefore, it was acceptable to assume that glacier meltwater flows directly into the lake, and infiltration of glacier meltwater is negligible.

Table 1 shows the volume of glacier meltwater estimated using the empirical formula. The glacier area was obtained from the glacial catalog dataset of China (Liu S et al., 2019). The average annual volume of glacier meltwater in 2010–2015 was considerably higher than that in 1980–2010 and indicates an acceleration of glacier retreat. The amount of glacier melt is mainly correlated with cumulative positive temperature (Zhang Y, 2006). Therefore, the volume of glacier meltwater in 2015–2020 was considered as the product between meltwater volume in 2010–2015 and a scaling factor, which was derived from cumulative positive daily air temperatures in 2010–2015 and 2015–2020.

(3) Actual evaporation over the land surface (E_a)

Over long timescales, change in water storage in a basin approaches zero (Patterson L et al., 2013). The average annual

runoff (R) is the difference between average annual precipitation (P) and average annual actual evaporation over the land surface (E_a). In addition, E_a can be estimated using the water-energy balance equation of the Budyko hypothesis (Choudhury B, 1999; Yang HB et al., 2008). According to the Budyko framework (Budyko M, 1974), lake water supplies and losses can be expressed as a function of the available water and energy; catchment properties and impacts of climate change can be separated analytically; the Budyko framework has been applied to different regions and basins worldwide because of its clarity and general applicability to hydrologic partitioning (Wang H et al., 2021).

$$R = P - E_a = P - \frac{P \times ET_0}{(P^n + {ET_0}^n)^{1/n}} \quad (3)$$

where n is a parameter that reflects the combined influences of various catchment properties such as soil, vegetation, and climate conditions. A larger n value is associated with a greater ratio of E_a to precipitation (Zhang SL et al., 2015).

3.3. Attribution analysis

Assuming that P, ET_0, and n are independent variables, Eq. (3) can be rewritten as $R= f (P, ET_0, n)$. To evaluate the sensitivity of runoff R to a climate variable x, Schaake J (1990) defined the climate elasticity of runoff as $\epsilon_x = \frac{\partial R/R}{\partial x/x}$. The elasticities of P, ET_0, and n were calculated as the reference (Xu XY et al., 2014), and derived the variation of R (dR) as follows:

$$dR = \Delta R_P + \Delta R_{ET_0} + \Delta R_n = \varepsilon_P \frac{R}{P} dP + \varepsilon_{ET_0} \frac{R}{ET_0} dET_0 + \varepsilon_n \frac{R}{n} dn \quad (4)$$

where ΔR_P, ΔR_{ET_0}, and ΔR_n are the runoff variations caused by the average annual changes of P, ET_0, and n between the base and impacted periods. Assuming that the relative error between the calculated value of $\Delta R_P+\Delta R_{ET_0}+\Delta R_n$ and the field measured value of dR is within acceptable limits, the contributions of P, ET_0, and n to runoff change η_i can be derived using $\eta_i = \frac{\Delta Ri}{dR}$.

4. Results and Discussion

4.1. Variations of the lake area and river runoff

Annual lake area and river runoff depth have significantly increased in recent decades (Figs. 3a–b). In the YHB, the lake area has been increasing at the rate of 4.6 km^2 per year; in the TRB, runoff depth has been increasing at the rate of 0.82 mm per year. The changes in the lake area of the YHB are comparable to those reported for the hinterland of the TP such as Linggoo Co (Lei Y et al., 2012), but much larger than those reported for the regions at the northeastern and southern edges of the TP such as Qinghai Lake (Li L et al., 2011) and Yamzhog Yumco Lake (Bian D et al., 2009). Using the Mann-Kendall (MK) test, the breakpoint was in found on the year of 2001 (significance level α=0.05; the critical value for the normal distribution $U_{\alpha/2}$=±1.96), which is consistent with previous studies (Lei Y et al., 2013).

To identify changes in lake volume and river runoff, the

Table 1. Glacier area and volume changes in the YHB.

Sub-basin	Glacier area/(S_g: km^2)			Glacier volume/(V_g: 10^8 m^3)			Glacier meltwater/(10^8 m^3)		
	1980	2010	2015	1980	2010	2015	1980–2010	2010–2015	2015–2020
Zhuonai	22.91	21.97	19.51	29.38	27.76	23.63	0.05	0.74	0.77
Kusai	39.67	37.73	36.70	61.88	57.81	55.68	0.12	0.38	0.40
Haiding Noir	0	0	0	0	0	0	0	0	0
Yanhu	7.26	7.09	6.97	6.18	5.99	5.85	0.01	0.02	0.03
The whole basin	69.84	66.79	63.18	97.45	91.56	85.16	0.18	1.15	1.19

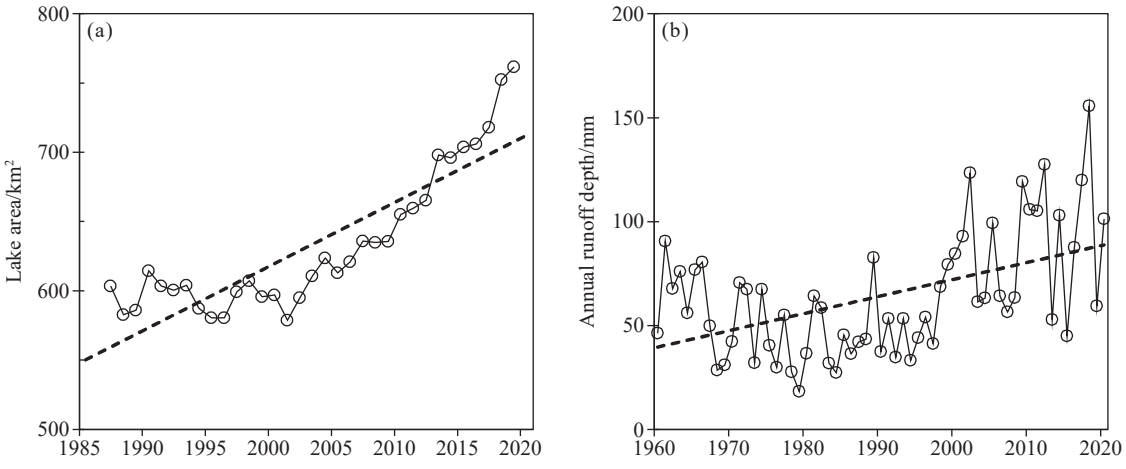

Fig. 3. Interannual variations of (a) lake area in the YHB, and (b) river runoff depth in the TRB.

statistical characteristics of precipitation, ET_0, and air temperature from 1960 to 2020 were examined (Table 2). The autocorrelation in both P and ET_0 was absent. In the YHB, P and ET_0 have been increasing at a rate of 23.12 mm/decade and 8.87 mm/decade, respectively. In the TRB, P and ET_0 have been increasing at rates of 11.21 mm/decade and 5.77 mm/decade, respectively. At the 95% confidence level, the P trend in the TRB is statistically significant while the ET_0 trend is not.

There was coherence between the positive trends of meteorological parameters, the lake area, and river runoff depth over recent decades, which indicates a remarkable intensification of the hydrological cycles in both YHB and TRB. For precipitation, the lake area, and river runoff, breakpoints were in the year 2001 (Fig. 4). Therefore, we refer to 1960–2000 as the base period and 2001–2020 as the impacted period.

4.2. Contribution to runoff increase

Table 3 shows the P, ET_0, and n elasticities of runoff increase in the TRB. Average annual ET_0, R, and P were all larger in the impacted period (T_2) than in the base period (T_1). However, n decreased from 1.02 in the base period to 0.91 in the impacted period. Moreover, the aridity index (ET_0/P) in the impacted period was 82% of that in the base period, which indicates that TRB was wetter in the impacted period than in the base period.

In addition, R was negatively correlated with ET_0 and n but positively correlated with P (Table 3). From the elasticities (ε), it showed that an increase of ET_0 by 10% during the base period was associated with a decrease of R by 8.4%; an increase of n by 10% was associated with a decrease of R by 21.4%; an increase of P by 10% was associated with an increase of R by 18.4%. For the impacted period, it suggested that an increase of ET_0 by 10% was associated with a decrease of R by 6.9%; an increase of n by 10% was associated with a decrease of R by 17.4%; an increase of P by 10% was associated with an increase of R by 16.9%. In terms of absolute values, precipitation elasticity (ε_P) was similar to n elasticity (ε_n) while evapotranspiration elasticity (ε_{ET_0}) was much smaller than ε_P and ε_n. These results indicate that runoff depth was more sensitive to changes in precipitation and n than to changes in potential evapotranspiration. Moreover, absolute elasticity values from the impacted period were slightly lower than those from the base period. These results suggest an increase in the sensitivity of runoff depth to changes in other factors, such as groundwater (Xu XY et al.,

Table 2. Results of Durbin-Watson (DW) tests and trend and breakpoint analyses of precipitation and potential evapotranspiration between 1960 and 2020 in both YHB and TRB.

Study area	Durbin-Watson (DW) Test	Variables	Annual average value	Changing trend β	Breakpoint year
YHB	–	P/mm	300.72	23.12**	2001
	–	ET_0/mm	767.56	8.87**	1996
TRB	–	P/mm	295.68	11.21*	2001
	–	ET_0/mm	863.96	5.77	1990

Note: Under Changing trend β, ** and * indicate statistical significance at the 99% and 95% confidence levels, respectively. Under Durbin-Watson (DW) Test, + and − denote autocorrelation and lack of autocorrelation (α=0.05), respectively.

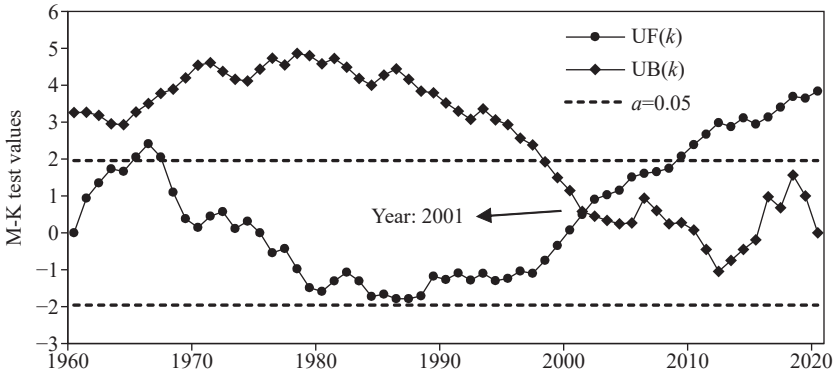

Fig. 4. Results of Mann-Kendall tests of runoff depths between 1960 and 2020 in the TRB.

Table 3. Precipitation (P), potential evapotranspiration (ET_0), and n elasticities of runoff (R) in the TRB for the base (T_1) and impacted (T_2) periods.

Period	R/mm	P/mm	ET_0/mm	n	R/P	ET_0/P	Elasticity coefficient		
							ε_P	ε_{ET_0}	ε_n
T_1	51.42	275.04	1208.02	1.02	0.19	4.39	1.84	−0.84	−2.14
T_2	90.35	337.98	1218.17	0.91	0.27	3.60	1.69	−0.69	−1.74
Change	38.93	62.93	10.15	−0.11	0.08	−0.79	−0.15	0.15	0.40

2014; Abera W et al., 2019).

The contributions of P, ET_0, and n to runoff depth change are shown in Table 4. The difference between the runoff depth change (dR') calculated using elasticities and the actual runoff depth change measured in the field (dR) was only 1.03 mm, and the relative error was 2.66%. These results indicate that the elasticity method used in this study can provide accurate quantitative assessments of the response of runoff change to climate change. The contribution of precipitation change to runoff depth change was approximately 24.41 mm, which represented 62.71% of the total runoff depth change. The contribution of change in n was approximately 13.90 mm, which represented 35.72% of the total runoff depth change. The contribution of ET_0 was approximately −0.42 mm, which represented −1.09% of the total runoff depth change. These results indicate that precipitation change was the main factor underlying the runoff change in the TRB between 1960 and 2020, and change in n was the second largest contributor.

4.3. Contributions to lake expansion

The monthly water level and area of Yanhu Lake have been monitored since 2015. The interannual changes in the volume of Yanhu Lake were 1.39, 1.81, 3.15, 7.83, and 4.61 Gt for 2015–2016, 2016–2017, 2017–2018, 2018–2019 and 2019–2020, respectively (Fig. 5a). Lake expansion has accelerated in recent years. The average annual change in the lake area was −0.45 km^2 in the base period (before 2001), 9.62 km^2 in the impacted period (2001–2020), and further increased to 11.56 km^2 during 2015–2020 (Fig. 5b). The lake water balance was calculated to explore the relative contributions of different elements to lake expansion.

The contributions of precipitation, land runoff, glacier meltwater, and groundwater to the variation of the lake water volume in the YHB during 2015–2020 using Eq. (1) (Table 5). Precipitation was the dominant lake water supply. It provided 84.35% of all lake water supplies in the form of direct precipitation over the lake surface (P: 24.44%) and land runoff as a result of precipitation (R_L: 59.91%). Glacier meltwater and groundwater provided 10.11% and 5.54% of all lake water supplies, respectively. In the YHB, glaciers cover 63.18 km^2 and account for 0.73% of the catchment area. These results are in close agreement with those reported for Siling Co where glaciers cover 0.63% of the catchment area

Table 4. Contributions of precipitation (P), potential evapotranspiration (ET_0) and n to runoff depth change in the TRB.

dR_P	dR_{ET_0}	dR_n	dR'	dR	Δ	Contribution ratio		
						η_P	η_{ET_0}	η_n
24.41	−0.42	13.90	37.89	38.93	−1.03	62.71	−1.09	35.72

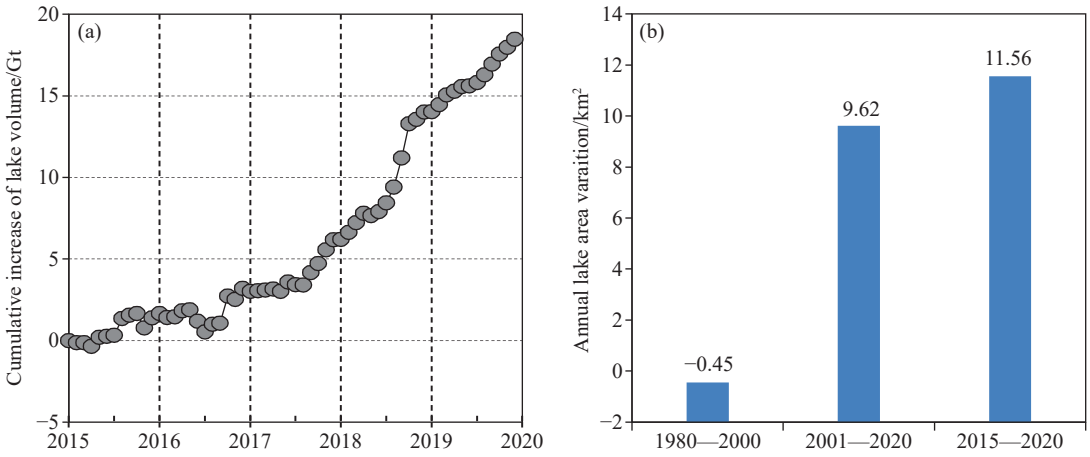

Fig. 5. a–Interannual variations of lake volume between 2015 and 2020; b–variations in an annual change of lake area for different periods between 1980 and 2020.

Table 5. The water balance between 2015 and 2020 in the YHB.

Periods	Supplies (10^8 m^3/a)					Losses/(10^8 m^3/a)	Variation (10^8 m^3/a)
	P	R_L	G	GW	Total	E	ΔV
2015–2016	2.03	6.11	1.02	0.54	9.70	8.32	1.39
2016–2017	2.46	5.36	1.35	0.48	9.66	8.11	1.54
2017–2018	2.81	6.18	1.19	0.56	10.74	7.76	2.98
2018–2019	3.57	10.13	1.30	0.96	15.95	8.12	7.83
2019–2020	3.48	7.40	1.08	0.71	12.67	8.07	4.61
2015–2020	2.87	7.04	1.19	0.65	11.75	8.08	3.67
proportion	24.44%	59.91%	10.11%	5.54%	100.00%	68.77%	31.23%

Note: The lake water supplies include precipitation over the lake water surface (P), precipitation-induced land runoff (R_L), glacier meltwater (G) and groundwater (GW); the lake water loss is the evaporation over the lake water surface (E).

and meltwater contributed to approximately 11.7% of lake level rise (Lei Y et al., 2013); this demonstrates the reliability of our results and suggests that groundwater and glacial meltwater play an influential role in lake expansion (Liu J et al., 2023), and may further impact on the fragile ecological environment fed by groundwater. Glaciers and permafrost are present in the basin of Yanhu Lake but absent from that of Qinghai Lake, which is located at the northeastern and southern edges of the TP. Consequently, the rate of expansion of Yanhu Lake is higher than that of Qinghai Lake.

Figure 6 shows the results of our water balance analysis and the water supplies and losses of the four lakes in the YHB. Assuming that Yanhu Lake is isolated from the three upstream lakes, the net volume increase in Yanhu Lake is 0.04 Gt. Assuming that the four lakes are connected, an inflow of 3.63 Gt from the upstream lakes into Yanhu Lake results in a net volume increase of 3.67 Gt. These results indicate that the large inflow from the upstream lakes was the key factor underlying the expansion of Yanhu Lake. As a result, some experts have suggested the necessity to enclose the upstream lakes by raising their natural levees to keep Yanhu Lake from overflowing. However, such large-scale engineering activities will cause considerable damage to the extremely fragile environment, flora, and fauna of the Hoh Xil region. More importantly, the results suggest that the overflow of Yanhu Lake was inevitable because the water balance of all four lakes was positive. Therefore, to protect areas downstream of Yanhu Lake from future flooding, it is recommended to divert water from Yanhu Lake into the lower Yangtze River.

4.4. Potential impacts on the ecological environment

To avoid great damage caused by the lake bank outburst, in August 2019, the competent department implemented the Yanhu Lake diversion project, diverting the lake water to the Qingshui River and eventually to the Chumar River, the northern source of the Yangtze River. The drainage project officially began operation at the end of August. The high salinity lake water diverted downstream will greatly impact the water quality of the source area of the Yangtze River and the stability of the permafrost base of the traffic corridor.

(i) Impact on the water quality of the source area of the Yangtze River

In October 2020, the water samples of Yanhu Lake, Qingshui River and Chumar River were collected respectively, in which S01 was Yanhu Lake water, S02 and S03 were water samples of Qingshui River before and after it was mixed with drainage water, and S04 and S05 were water samples of Chumaer River before and after it was mixed with drainage water (Fig. 7). The test results are shown in Table 6. The Yanhu Lake water is Cl-Na type with high salinity, which results in the impact on the downstream water quality mainly manifested in the increase of salt. Before and after drainage, the total dissolved solids (TDS) of Qingshui River water increased from 992 mg/L to 13432 mg/L, and that of Chumaer River increased from 2689 mg/L to 5384 mg/L, and the increase of TDS was mainly caused by the increase of Na^+ and Cl^-, accounting for about 90% (Fig. 8). Inorganic toxicological components and toxic heavy metal components almost did not change, which were less than the detection limit and far below the standard of drinking water quality. However, the significantly increased salinity in the source region of the Yangtze River can also lead to changes in the composition and distribution of biological species.

(ii) Impact on downstream Qinghai-Tibet Highway (Railway)

The upper depth of permafrost in this area is 2–5 m, and the thickness of permafrost is 20–60 m. It is the main supporting layer of the pier foundation of the Qingshuihe Bridge of the Qinghai-Tibet Railway in this area. This area is

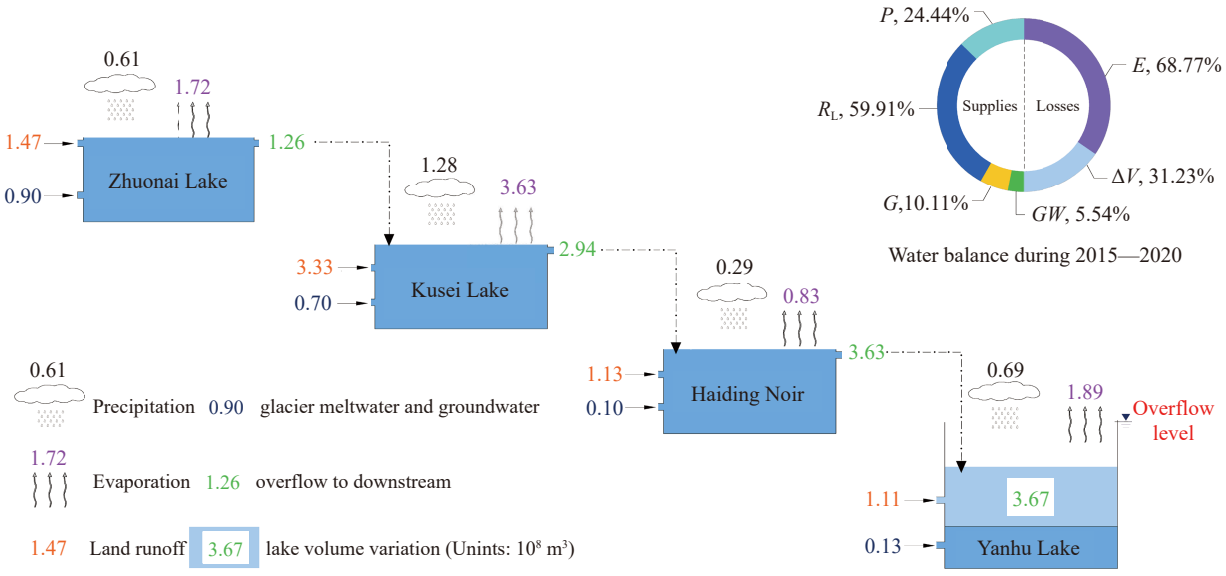

Fig. 6. The water balance of the four lakes between 2015 and 2020 in the YHB. The pie chart shows the whole basin's average water balance in 2015–2020.

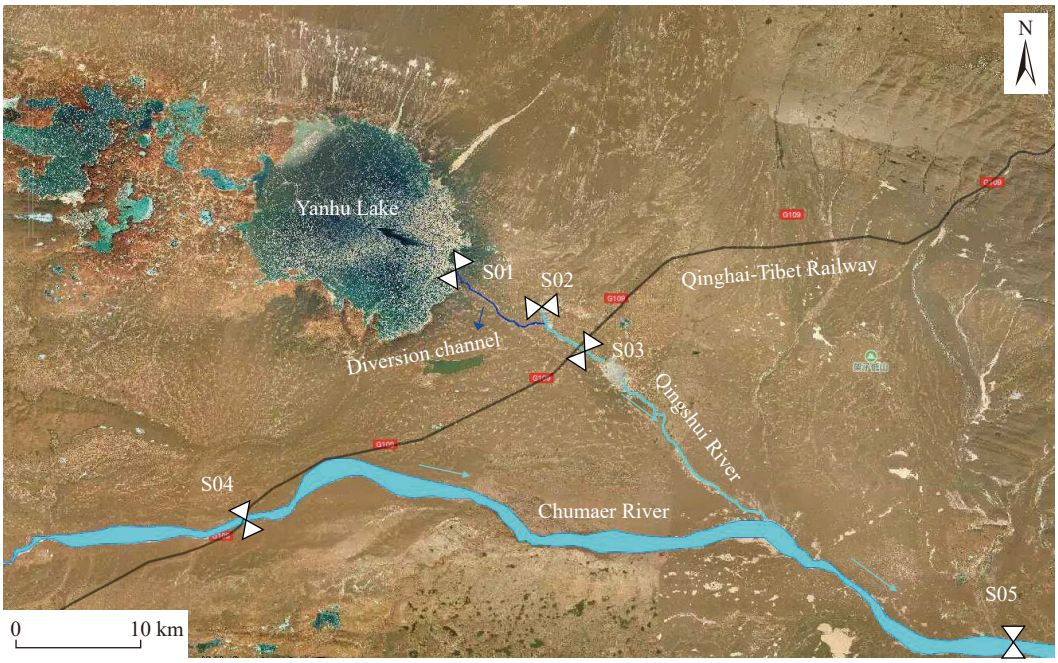

Fig. 7. The spatial distribution of the water samples.

Table 6. The ion concentrations (mg/L) of the river and lake water.

Classification		S01	S02	S03	S04	S05
General chemical components	pH	8.9	7.56	8.85	8.03	8.35
	K^+	81.56	5.91	82.57	11.25	27.56
	Ca^{2+}	16.85	124.6	11.88	86.48	53.95
	Mg^{2+}	467.9	67.35	481.2	62.27	164.2
	SO_4^{2-}	733.1	120.0	792.4	357.3	438.9
	HCO_3^-	535.8	485.1	549.8	165.2	262.1
	CO_3^{2-}	215.8	0	198	0	29.97
	Fe	<0.010	0.27	<0.010	0.397	0.071
	Mn	<0.001	0.082	<0.001	0.08	0.082
	Cu	<0.010	<0.010	<0.010	<0.010	<0.010
	Zn	<0.002	0.01	<0.002	<0.002	<0.002
	Al^{3+}	<0.02	0.03	<0.02	<0.02	<0.02
	NH_4^+	<0.04	0.08	<0.04	<0.04	<0.04
	H_2SiO_3	<1.00	36.54	1.23	2.49	3.08
	HBO_2	55.36	1.82	58.2	2.54	15.82
Inorganic toxicological components	NO_3^-	1.73	0.72	1.52	1.82	1.45
	NO_2^-	<0.002	<0.002	<0.002	<0.002	<0.002
	F^-	0.41	0.82	0.31	0.3	0.36
	I^-	<0.02	<0.02	<0.02	<0.02	<0.02
Toxic heavy metal components	As	0.014	0.004	0.013	0.002	0.003
	Pb	<0.001	<0.001	<0.001	0.002	<0.001
	Cr^{6+}	<0.004	<0.004	<0.004	0.004	<0.004
	Cd	<0.0005	<0.0005	<0.0005	<0.0005	<0.0005
	Hg	<0.0001	<0.0001	<0.0001	<0.0001	<0.0001

located at the edge of a high-temperature unstable permafrost region, the annual average ground temperature of permafrost is close to −0.5°C (Cheng GD et at al. 2019), and it is afraid of heat, water and salt, which is easily to disturbed to produce uneven thermal melt erosion damage. Friction piles of 18–30 m in length is used for the bridge pier foundation and placed in the frozen soil layer. The Yanhu Lake water shows high salinity and strong corrosion. Under the action of lake water erosion and thermal melt erosion for a long time, it will cause the channel cut down, accelerate the uneven melting of

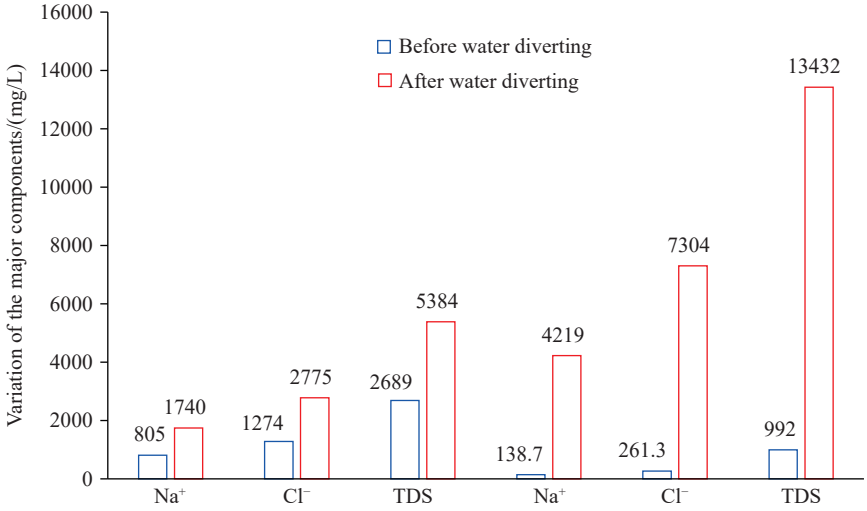

Fig. 8. Significant changed components of the water in Qingshui River and Chumaer River before and after diversion.

permafrost, and produce negative friction resistance and corrosion effect on the pier foundation, which may lead to the uneven settlement of pier, tilt, concrete erosion and other diseases. Therefore, the diverted water may affect the normal operation of Qingshuihe Bridge on the Qinghai-Tibet Railway.

There is a culvert on the Qinghai-Tibet Highway with a cross-section of 10.89×2.10 m^2 (Fig. 9). If the water discharged from Yanhu Lake exceeds the water crossing capacity of the culvert by 17–20 m^3/s, the highway will be flooded and even the subgrade will be destroyed. However, the drainage flow in October and November, 2019 was 23.5 m^3/s and 30.1 m^3/s respectively, both exceeding the water crossing capacity of the culvert. Therefore, if no measures are taken, the Qinghai-Tibet Highway will be paralyzed. To ensure the normal operation of the Qinghai-Tibet Highway, Authorities had already built a new bridge over the Qinghai-Tibet Highway to replace the small culvert before the diversion operation.

5. Conclusions

The key findings of this study are:

(i) Using the Budyko framework, the contributions of changes in precipitation, potential evapotranspiration, and underlying catchment properties to runoff change were quantified in both YHB and TRB. The hydrological cycles in the study area have intensified under climate change; precipitation, the lake area, and river runoff have increased. The main replenishment source of lake expansion was precipitation, followed by glacier meltwater and groundwater.

(ii) The overflow of Yanhu Lake was inevitable because the water balance of all four lakes was positive and the four lakes were connected. To protect areas downstream of Yanhu Lake from future flooding, it was recommended diverting water from Yanhu Lake into the lower Yangtze River rather than enclosing the upstream lakes by raising their natural levees considering the positive water balance and the need to protect the fragile local environment.

(iii) The Yanhu Lake water is Cl-Na type with a salinity of 13.4 g/L. After the lake water is diverted to the Yangtze River, the salinity of the water in the downstream Qingshui River and Chumaer River will be significantly increased, but the inorganic toxicological and heavy metal components were almost unchanged. In addition, it will affect the stability of the permafrost subgrade of the Qingshui River Bridge of the Qinghai-Tibet Railway, and the water capacity of the original Qinghai-Tibet Highway culver cannot meet the drainage requirements. A new Qingshui River highway bridge with greater water crossing capacity is needed.

CRediT authorship contribution statement

Chang-chang Fu and Xiang-quan Li conceived of the presented idea. Chang-chang Fu wrote the manuscript in consultation. Xu Cheng provided the necessary data. All authors discussed the results and contributed to the final manuscript.

Declaration of competing interest

The authors declare no conflicts of interest.

Acknowledgment

This work was funded by the National Natural Science Foundation of China (42002264), the China Geological Survey Program (DD20230537), and the Fundamental Research Funds for the Central Public Research Institutes (SK202006). The authors are grateful to Dr. Ai-min Wu, Dr. Yong-shuang Zhang, Dr. Jing-tao Liu, Dr. Peng He and three anonymous reviewers for their constructive comments and suggestions which substantially improved this work in science and presentation. The authors also thank Tina Tin, Ph.D., from Liwen Bianji (Edanz) (www.liwenbianji.cn/), for editing the English text of a draft of this manuscript.

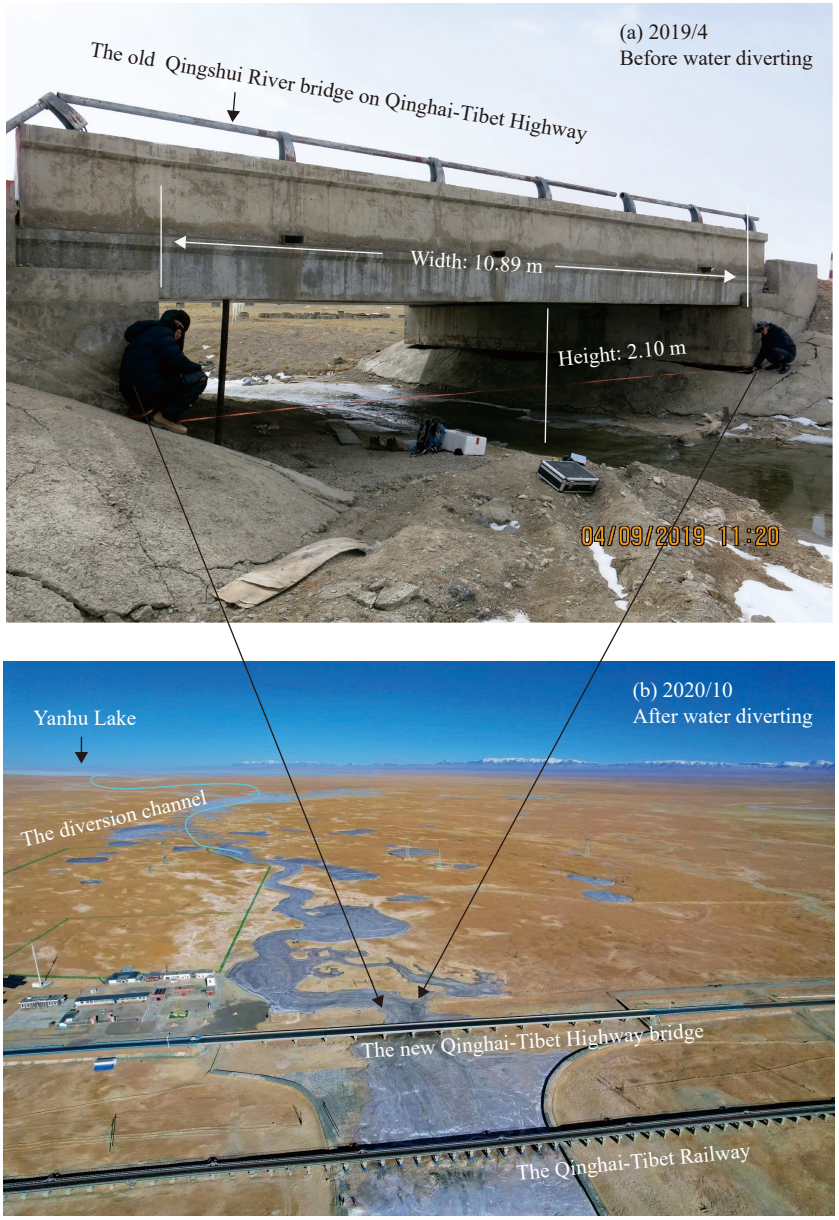

Fig. 9. Changes of the Qingshui River bridge before and after Yanhu Lake water diverting. a–The old bridge is quite narrow and has limited water crossing capacity; b–after the demolition of the old bridge, the modern Qingshui River Bridge was built to ensure the safety of the Qinghai-Tibet highway through which the Yanhu Lake water is diverted.

References

Abera W, Tamene L, Abegaz L, Solomon D. 2019. Understanding climate and land surface changes impact on water resources using Budyko framework and remote sensing data in Ethiopia. Journal of Arid Environments, 167, 56–64. doi: 10.1016/j.jaridenv.2019.04.017.

Abdollah P, Mohammad G, Hamid D, Jan A, Sajad R. 2019. Using the Mann-Kendall test and double mass curve method to explore stream flow changes in response to climate and human activities. Journal of Water and Climate Change, 10, 725–742. doi: 10.2166/wcc.2018.162.

Allen RG, Jensen ME, Wright JL, Burman RD. 1989. Operational estimates of reference evapotranspiration. Agronomy Journal, 81(4), 650–662. doi: 10.2134/agronj1989.00021962008100040019x.

Biskop S, Maussion F, Krause P, Fink M. 2015. What are the key drivers of regional differences in the water balance on the Tibetan Plateau? Hydrology & Earth System Sciences Discussions, 12, 4271–4314. doi: 10.5194/hessd-12-4271-2015.

Bian D, Du J, Hu J, Li C, Li L. 2009. Response of the water level of the Yamzho Yumco to climate change during 1975–2006. Journal of Glaciology and Geocryology, 31, 404–409 (in Chinese with English abstract).

Budyko M. 1974. Climate and Life. Academic Press, New York, USA, 508. doi: 10.1016/0019-1035(76)90196-2.

Chen DL, Xu QB, Yao TD, Guo ZT, Cui P, Chen FH, Zhang RH, Zhang XZ, Zhang YL, Pan J, Hou ZQ, Zhang TH. 2015. Assessment of past, present and future environmental changes on the Tibetan Plateau. Chinese Science Bulletin, 60(32), P3025–3037. doi: 10.1360/n972014-01370.

Cheng GD, Zhao L, Li R, Wu XD, Sheng Y, Hu GJ, Zou DF, Jin HJ, Li X, Wu QB. 2019. Characteristic, changes and impacts of permafrost on Qinghai-Tibet Plateau. Chinese Science Bullition, 64, 2783–2795. doi: 10.1360/TB-2019-0191.

Choudhury B. 1999. Evaluation of an empirical equation for annual evaporation using field observations and results from a biophysical model. Journal of Hydrology, 216, 99–110. doi: 10.1016/S0022-1694(98)00293-5.

Immerzeel WW, Beek V, Bierkens M. 2010. Climate change will affect the Asian Water Towers. Science, 328(5984), 1382–1385. doi: 10.1126/science.1183188.

Lei Y, Yao T, Yi C, Wang W, Sheng YW, Li J, Joswiak D. 2012. Glacier mass loss induced the rapid growth of Linggo Co on the central Tibetan Plateau. Journal of Glaciology, 58, 177–184. doi: 10.3189/2012JoG11J025.

Lei Y, Yao T, Bird B, Yang K, Zhai J, Sheng Y. 2013. Coherent Lake growth on the central Tibetan Plateau since the 1970s: Characterization and attribution. Journal of Hydrology, 483, 61–67. doi: 10.1016/j.jhydrol.2013.01.003.

Li L, Shi XH, Shen HY, Dai S, Xiao JS. 2011. Cause of water level fluctuation in Qinghai Lake from 1960 to 2009 and its future trend forecasting. Journal of Natural Resources, 26, 1566–1574 (in Chinese with English abstract).

Liu S, Guo W, Xu J. 2019. The second glacial catalogue data set of China (v1.0). National glacial and frozen desert scientific data center (in Chinese with English abstract).

Liu J, Cheng YP, Zhang FE, Wen XR, Yang L. 2023. Research hotspots and trends of groundwater and ecology studies: Based on a bibliometric approach. Journal of Groundwater Science and Engineering, 11(1), 20–36. doi: 10.26599/JGSE.2023.9280003.

Mukhtar MA. 1987. Durbin-Watson and generalized Durbin-Watson tests for autocorrelations and randomness. Journal of Business and Economic Statistics, 5, 195–203. doi: 10.1080/07350015.1987.10509578.

Otsu N. 1979. A threshold selection method from gray-level histograms. IEEE Trans Syst Man Cybern SMC, 9, 62–66. doi: 10.1109/TSMC.1979.4310076.

Patterson L, Lutz B, Doyle M. 2013. Climate and direct human contributions to changes in mean annual streamflow in the South Atlantic, USA. Water Resources Research, 49, 7278–7291. doi: 10.1002/2013WR014618.

Penman HL. 1948. Natural evaporation from open water, bare soil and grass. Proc. Roy. Soc. Of London, Ser.193, 120–145.

Pritchard HD. 2019. Asia' s shrinking glaciers protect large populations from drought stress. Nature, 569, 649–654. doi: 10.1038/s41586-019-1240-1.

Qiao BJ, Zhu LP. 2019a. Difference and cause analysis of water storage changes for glacier-fed and non-glacier-fed lakes on the Tibetan Plateau. Science of the Total Environment, 693, 33399. doi: 10.1016/j.scitotenv.2019.07.205.

Qiao BJ, Zhu LP, Yang RM. 2019b. Temporal-spatial differences in lake water storage changes and their links to climate change throughout the Tibetan Plateau. Remote Sensing of Environment, 222, 2–243. doi: 10.1016/j.rse.2018.12.037.

Rosenberry D, Winter T, Buso D, Likens G. 2007. Comparison of 15 evaporation methods applied to a small mountain lake in the northeastern USA. Journal of Hydrology, 340, 149–166. doi: 10.1016/j.jhydrol.2007.03.018.

Schaake J. 1990. From climate to flow. John Wiley and Sons Inc:New York, USA, 177–206.

Sen PK. 1969. Estimates of the regression coefficient based on Kendall's tau. Journal of the American Statistical Association, 63, 1379–1389. doi: 10.1080/01621459.1968.10480934.

Shi YF, Shen YP, Li DL, Zhang GW, Ding YJ, Hu RJ, Kang ES. 2003. Discussion on the present climate change from warm-dry to warm-wet in northwest China. Quaternary Science, 23, 152–164 (in Chinese with English abstract).

Wang C, Dai CL, Song CJ. 2022. Analysis of the temporal and spatial distribution characteristics of climate change in the Qinghai-Tibetan Plateau. Yellow River, 44(9), 6–82 (in Chinese with English abstract).

Wang H, Lv X, Zhang M. 2021. Sensitivity and attribution analysis based on the Budyko hypothesis for streamflow change in the Baiyangdian catchment, China. Ecological Indicators, 121, 1470–160X. doi: 10.1016/j.ecolind.2020.107221.

Wang LC, Yu K, Chang L, Zhang J, Tang T, Yin LH, Gu XF, Dong JQ, Lia Y, Jiang J, Yang BC, Wang Q. 2021. Response of glacier area variation to climate change in the Kaidu-Kongque river basin, Southern Tianshan Mountains during the last 20 years. China geology, 3, 389–401. doi: 10.31035/cg2021055.

Wu QB, Niu FJ. 2013. Permafrost changes and engineering stability in Qinghai-Tibet Plateau. Chinese Science Bulletin, 58(2), 15–130 (in Chinese with English abstract).

Xu XY, Yang DW, Yang HB, Lei HM. 2014. Attribution analysis based on the Budyko hypothesis for detecting the dominant cause of runoff declines in Haihe basin. Journal of Hydrology, 510, 530–540. doi: 10.1016/j.jhydrol.2013.12.052.

Yang HB, Yang DW, Lei ZD, Sun FB. 2008. New analytical derivation of the mean annual water-energy balance equation. Water Resources Research, 44, 893–897. doi: 10.1029/2007WR006135.

Yao XJ, Sun MP, Gong P, Liu BK, Li XF, An LN, Yan LX. 2018. Overflow probability of the Salt Lake in Hoh Xil Region. Acta Geographica Sinica, 28, 647–655. doi: 10.1007/s11442-018-1496-7.

Yao TD, Thompson L, Mosbrugger V, Zhang F, Ma YM, Luo TX, Xu BQ, Yang XX, Joswiak DR, Wang WC, Joswiak ME, Devkota LP, Tayal S, Jilani R, Fayziev R. 2012. Third Pole Environment (TPE). Environmental Development, 3, 52–64. doi: 10.1016/j.envdev.2012.04.002.

Yao TD, Xue YK, Chen DL, Chen FH, Thompson L, Cui P, Koike T, Lau WKM, Mosbrugger V. 2019. Recent Third Pole's rapid warming accompanies cryospheric melt and water cycle intensification and interactions between monsoon and environment: multi-disciplinary approach with observation, modeling and analysis. Bulletin of the American Meteorological Society, 100(3), 423–444. doi: 10.1175/BAMS-D-17-0057.1.

Yu C, Wu LJ, Zhang YL, Wang XY, Wang ZC, Zhang Z. 2022. Effect of groundwater on the ecological water environment of typical inland lakes in the Inner Mongolian Plateau. Journal of Groundwater Science and Engineering, 10(4), 353–366. doi: 10.19637/j.cnki.2305-7068.2022.04.004.

Zhang GQ, Yao TD, Shum CK, Yi S, Yang K, Xie HJ, Feng W, Bolch T, Wang L, Behrangi A. 2017. Lake volume and groundwater storage variations in Tibetan Plateau 's endorheic basin. Geophysical Research Letters, 44, 5550–5560. doi: 10.1002/2017GL073773.

Zhang GQ, Yao TD, Chen WF, Zheng GX, Shum CK, Yang K, Piao SL, Sheng YW, Yi S. 2019. Regional differences of lake evolution across China during 1960s-2015 and its natural and anthropogenic causes. Remote Sensing of Environment, 221, 386–404. doi: 10.1016/j.rse.2018.11.038.

Zhang Y, Liu S, Ding Y. 2006. Observed degree-day factors and their spatial variation on glaciers in western China. Annals of Glaciology, 43, 301–306. doi: 10.3189/172756406781811952.

Zhang SL, Yang HB, Yang DW, Jayawardena AW (2015). Quantifying the effect of vegetation change on the regional water balance within the Budyko Framework. Geophysical Research Letters 43 (3), 1140–1148. doi: 10.1002/2015GL066952.

Zhou J, Wang L, Zhang YS, Guo YH, Li XP, Liu WB. 2015. Exploring the water storage changes in the largest lake (Selin Co) over the Tibetan Plateau during 2003–2012 from a basin-wide hydrological modeling. Water Resources Research, 51, 8060–8086. doi: 10.1002/2014WR015846.

Zhu L, Yang MN, Liu JT, Zhang YX, Chen X, Zhou B. 2022. Evolution of the freeze-thaw cycles in the source region of the Yellow River under the influence of climate change and its hydrological effects. Journal of Groundwater Science and Engineering, 10(4), 322–334. doi: 10.19637/j.cnki.2305-7068.2022.04.002.